
Article:
Tang, Zhichuan, Yu, Hongnian, Lu, Chunfu et al. (2 more authors) (2019) Single-Trial Classification of Different Movements on One Arm Based on ERD/ERS and Corticomuscular Coherence. IEEE Access. pp. 128185-128197. ISSN 2169-3536

https://doi.org/10.1109/ACCESS.2019.2940034

Received August 21, 2019, accepted August 28, 2019, date of publication September 9, 2019, date of current version September 20, 2019.

Digital Object Identifier 10.1109/ACCESS.2019.2940034

Single-Trial Classification of Different Movements on One Arm Based on ERD/ERS and Corticomuscular Coherence

ZHICHUAN TANG[1], (Member, IEEE), HONGNIAN YU[2], CHUNFU LU[1], PENGCHENG LIU[3], (Member, IEEE), AND XUEXUE JIN[1]

[1]Industrial Design Institute, Zhejiang University of Technology, Hangzhou 310023, China
[2]School of Engineering and the Built Environment, Edinburgh Napier University, Edinburgh EH10 5DT, U.K.
[3]Cardiff School of Technology, Cardiff Metropolitan University, Cardiff CF5 2Y, U.K.

Corresponding author: Zhichuan Tang (ztang@zjut.edu.cn)

This work was supported in part by the National Natural Science Foundation of China under Grant 61702454 and Grant 61803396, in part by the Ministry of Education in China (MOE) Project of Humanities and Social Sciences under Grant 17YJC870018, in part by the Fundamental Research Funds for the Provincial Universities of Zhejiang under Grant GB201901006, and in part by the Key Research and Development Program of Zhejiang Province under Grant 2019C03124.

ABSTRACT Electroencephalography (EEG)-based brain-machine interface (BMI) is widely applied to control external devices like a wheel chair or a robotic arm, to restore motor function. EEG is useful to distinguish between left arm and right arm movements, however, it is difficult to classify the different movements on one arm. In this paper, a two-step single-trial classification method is proposed to recognize three movements (make a fist, hand extension and elbow flexion) of left and right arms: (1) distinguish between left arm and right arm movements by decoding event-related (de) synchronization (ERD/ERS) and (2) recognize the specific movement of this arm using corticomuscular coherence as features. Four healthy subjects are employed in a cue-based motor execution (ME) experiment. In Step one, ERD and post-movement ERS are found over the contralateral sensorimotor area; in Step two, for each movement, only the beta-band coherence between C3/C4 and the corresponding agonistic muscle is significant. The classification results show the best accuracy of Step one and Step two is 88.10% and 93.33%, respectively. This proposed method achieves a total accuracy of 82.22%. This study demonstrates that our method is effective to classify different movements on one arm, and provides the theoretic basis and technical support for the practical development of BMI-based motor restoration applications.

INDEX TERMS Arm movement classification, BMI, EEG-EMG coherence, ERD/ERS, motor restoration.

I. INTRODUCTION

As a direct means of communication combining human brain with the external devices, the electroencephalography (EEG)-based brain-machine interface (BMI) can be considered as being the main way of communication for people affected by motor disabilities [1]–[3]. Some external devices such as wheel chair, robotic arm and neuroprosthetics, are controlled by BMI to restore motor function [4]–[8]. Bypassing the conventional neural muscular conduction pathway, human motion intentions can be decoded directly into machinery commands through BMI [9]. This helps patients with neuromuscular disorder to restore motor function and regain their independence in daily life [10], [11].

The associate editor coordinating the review of this manuscript and approving it for publication was Jing Liang.

EEG signals' low signal-to-noise ratio is the main reason to lead to a low decoding accuracy for EEG-based BMI applications [12]. When we collect the EEG signals through surface electrodes placed on the scalp, the noise levels are increased because of multiple artefacts (motion of electrodes and cables, gel drying, electrode polarization, etc.). To this problem, lots of previous studies have focused on looking for reliable features and pattern recognition algorithms to improve the classification accuracy of EEG signals [13], [14]. Event-related (de) synchronization (ERD/ERS) patterns [15] have been considered as important features to distinguish between left hand and right hand movements, according to the attenuation/increase phenomenon of EEG amplitude during motor imagery (MI) or motor execution (ME) [16], [17]. Pfurtscheller *et al.* [18] found the ERD/ERS features in alpha frequency bands (9-14 Hz) and beta frequency bands

0 could be used to distinguish between left hand and right hand motor imageries, and the online classification accuracy was approximately 80% in all 3 subjects. Huang *et al.* [19] observed the ERD/ERS over the contralateral sensorimotor area to the hand movements for both MI and ME, and the offline classification accuracy was as high as 88%. To date, ERD/ERS features have been applied in cursor, wheel chair and neuroprosthetics control as well. The classification accuracy of left hand and right hand movements in some of these researches has been close to 90% [20], [21].

EEG is useful to distinguish between left hand and right hand movements, however, it is difficult to classify the different movements on one arm. Due to the complexity of upper limb movements in daily life, how to recognize motion intention of one arm is especially important, which could make the neuroprosthetics and robotic arm assist daily life of users effectively [22]–[24]. For this reason, some researchers have focused on the classification of different movements on one arm using EEG signals, but the classification accuracy is still less than 50% resulting from the limited spatiotemporal resolution [25]. Therefore, using EEG signals only is hard to improve the classification accuracy of different movements on one arm. Corticomuscular coherence (CMC) measured between EEG and electromyography (EMG) helps to understand the cortical control for limb movements [26]. When a muscle contracts, a functional coupling relationship exists between the contralateral sensorimotor cortex and this muscle in several different frequency bands [27], [28]. So EEG-EMG coherence can be used as the feature to classify different movements. Most previous researches used EEG-EMG coherence to understand the corticomuscular functional connection [29], [30]. To the best of our knowledge, EEG-EMG coherence has not been applied as a feature in classification of movements on one arm yet.

This study aims to use a novel BMI paradigm to classify different movements on one arm. In this paradigm, a two-step single-trial classification method is proposed to recognize three movements (make a fist, hand extension and elbow flexion) of left and right arms: (1) distinguish between left arm and right arm movements by decoding ERD/ERS and (2) recognize the specific movement of this arm using EEG-EMG coherence as features. Advanced feature extraction and classification algorithms were used for single-trial EEG signal processing. Then we tested whether this proposed method is reliable enough to decode different motion intentions of one arm.

II. MATERIAL AND METHODS

A. SUBJECTS

4 healthy 25- to 30-year-old subjects (3 males and 1 female, all right handed according to the Edinburgh inventory [31]) participated in our experiment. Before the experiment, all subjects signed the informed consents, and let them know the experimental procedure. The ethical clearance committee of Zhejiang University reviewed the experimental protocol and approved it.

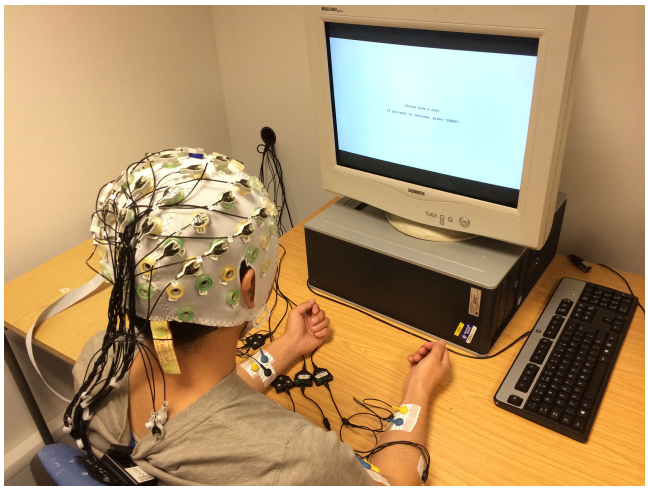

FIGURE 1. One subject in the experiment. After the EEG electrodes and EMG electrodes were attached and all signals were normal, subjects sit before the screen, and kept their forearms semi-extended and palms supinated. Both shoulders and all fingers were relaxed. To maintain the attention level of subjects during recording, a quiet and dim-light experimental environment was provided.

B. EXPERIMENTAL PARADIGM

After the EEG electrodes and EMG electrodes were attached and all signals were normal, subjects sat before the screen, and kept their forearms semi-extended and palms supinated (see Figure 1). Both shoulders and all fingers were relaxed. To maintain the attention level of subjects during recording, a quiet and dim-light experimental environment was provided. In addition, some unnecessary movements such as blinks, eye movements and body movements should be avoided after the visual cue. A 19-inch CRT screen was used to present the visual cues with a 1.2° visual angle.

In this ME experiment, each subject completed totally 360 trials (random sequences of 60 trials × 6 movements, see Table 1). Each trial lasted 7 seconds [17], and the timing of one trial is shown in Figure 2. A beep sound and a cross at second 2 meant the start of this trial. Then, at second 3, a visual cue selected in one of six (a left/right arrow and a word) appeared in the center of the screen. The six different cues were "←fist", "←hand", "←elbow", "→fist", "→hand" and "→elbow", which indicated the different movements: make a left fist, left-hand extension, left-elbow flexion, make a right fist, right-hand extension and right-elbow flexion, respectively. Subjects performed the ME naturally for 4 seconds, until the cue disappeared at second 7. After a random duration (2-5 seconds) for short pause, the next trial would start.

Subjects started movements immediately when the cue appeared in each trial, and were instructed to have a 10-min rest between every 60 trials to avoid mental or muscle fatigue [32]. To avoid body movements and fatigue during the 60 trials, we took two actions: (1) a camera was used to observe subjects to ensure that they did not make unnecessary movements (eye or tongue movements) after the

TABLE 1. The descriptions of six movements in this study.

Class	Movement	Description	Cue
Class 1	Make a left fist	Make a left fist naturally, and keep right arm semi-extended and right palm supinated.	"←fist"
Class 2	Left-hand extension	Extend left hand fully, and keep right arm semi-extended and right palm supinated.	"←hand"
Class 3	Left-elbow flexion	Flex left elbow at a steady speed, and keep right arm semi-extended and right palm supinated.	"←elbow"
Class 4	Make a right fist	Make a right fist naturally, and keep left arm semi-extended and left palm supinated.	"→fist"
Class 5	Right-hand extension	Extend right hand fully, and keep left arm semi-extended and left palm supinated.	"→hand"
Class 6	Right-elbow flexion	Flex right elbow at a steady speed, and keep left arm semi-extended and left palm supinated.	"→elbow"

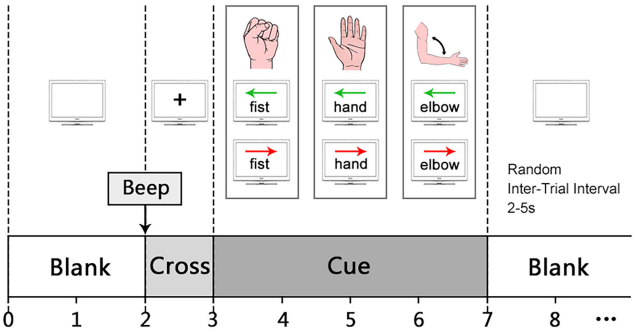

FIGURE 2. Timing of the BMI paradigm used in the experiment. A beep sound and a cross at second 2 meant the start of this trial. Then, at second 3, a visual cue selected in one of six (a left/right arrow and a word) appeared in the center of the screen, which indicated the different movements. Subjects performed the ME naturally for 4 seconds, until the cue disappeared at second 7. After a random duration (2-5 seconds) for short pause, the next trial would start.

cue appearance, performed movements correctly, and were attentive and awake; (2) median frequency (MF, a frequency domain feature of EMG) of muscles of left and right arms were observed to avoid muscle fatigue. A decrease of MF means muscle fatigue [33]. Additionally, they could have a break anytime during the experiment if they were too fatigued to continue the arm movements. The duration of experiment for each subject was approximately 2.5 hours.

C. TRIAL EXCLUSION

We identified all trials offline, and excluded the trials including the EEG artifacts of blinks, eye movements or body movements from the following analyses. For EMG recordings, trials that contained bilateral movements (EMG activities in both arms) were excluded.

D. DATA ACQUISITION

28 EEG channels (P6, P4, P2, Pz, P1, P3, P5, CP6, CP4, CP2, CPz, CP1, CP3, CP5, C6, C4, C2, Cz, C1, C3, C5, FC6, FC4, FC2, FCz, FC1, FC3, FC5) were selected to collect EEG signals using an EEG cap connecting with an actiCHamp EEG signal amplifier (Brain Products, Gilching, Germany). The placements of reference electrode and ground electrode were at left mastoid and position Fz, respectively. After wearing the cap, conductive gel was used to reduce impedance between electrodes and scalp. According to the recorder software (Brain Vision), electrode impedance was visually observed to keep lower than 5 kΩ. EEG signals were low-pass filtered at 100 Hz, high-pass filtered at 0.5 Hz, and sampled at 500 Hz. A 50-Hz notch filter was set to remove line interference.

EMG data were collected from digitorum superficialis, extensor digitorum and biceps brachii of both left and right arms, corresponding to the agonistic muscle of three movements: make a fist, hand extension and elbow flexion, respectively [34], [35]. Six MyoScan EMG sensors (Thought Technology Ltd., Canada) were used for six muscles' EMG recordings. Sensors' main parameters include: measuring range is 0-2000 μV, input impedance is higher than 10 kΩ, CMRR is higher than 130 dB, and input/output gain is 500. Before attaching the electrodes, alcohol and conductive gel were used to clean the skin and reduce impedance between electrodes and skin, respectively. Six EMG sensors with triode electrodes were placed on the midline of the muscle belly of targeted muscles according to [36]. The inter-electrode distance was 2 cm. EMG signals were low-pass filtered at 150 Hz, high-pass filtered at 5 Hz, and sampled at 500 Hz. A 50-Hz notch filter was set to remove line interference.

MATLAB R2017a (MathWorks, Inc., Natick, USA) was used to calculate and analysis all data in the experiment.

E. FEATURE EXTRACTION AND CLASSIFICATION

In this paper, we proposed a two-step single-trial classification method to classify different movements on one arm: (1) distinguish between left and right arm movements by decoding ERD/ERS and (2) recognize the specific movement of this arm using EEG-EMG coherence as features. The procedure of feature extraction and classification of two steps were as follows.

1) STEP ONE: DISTINGUISH BETWEEN LEFT AND RIGHT ARM MOVEMENT

- *ERD/ERS visualizations:*
  The collected EEG signals were filtered at 8-30 Hz (alpha and beta frequency bands) which includes most important movement information [18]. All movements were divided into two classes (Class L and Class R), i.e. left arm movement (Class 1-3) and right arm movement (Class 4-6). For Class L and Class R, EEG power of C3 and C4 channels within two frequency bands (8-12 Hz and 14-30 Hz) during 0-7 s were averaged over

all trials and all subjects. The ERD/ERS curves are calculated as a percentage of EEG power decrease/increase relative to the reference period (0.5-1.5 s in this experiment) [15], according to the equation below

$$ERD/ERS\% = (P - R)/R \times 100, \tag{1}$$

where P is the EEG power of targeted period, and R is the EEG power of reference period. Grand average topographies based on ERD/ERS curves and time-frequency maps generated by fast Fourier transformation (FFT) with 100-ms Hanning windows were used to visualize ERD/ERS patterns [37].

- *Feature extraction:*
By referring to the ERD/ERS curves and time-frequency maps, the best time period and frequency band for each subject were chosen to gain the strongest ERD/ERS. The selected time period was windowed by 200-ms time segments to extract features. As a general algorithm, common spatial pattern (CSP) was used in our experiment for feature extraction, which calculated spatial filters for discrimination between two brain states (corresponding to Class L and Class R) successfully [38]. In order to find the optimal spatial filters, the CSP algorithm can maximize variance differences between two classes to obtain highly distinguishable features [39]. Each trial's EEG data were transformed into a $C \times N$ matrix M, where C represents the channel numbers (28 channels in this study) and N represents the sample numbers per channel. The normalized covariance matrix is

$$Cov = MM'/trace(MM'), \tag{2}$$

where $'$ means the transpose of this matrix, and $trace(x)$ is the sum of the diagonal elements of x. For each class, the averaged covariance matrix $\overline{Cov}$ is given by averaging all trials of this class (Class L or Class R). The composite spatial covariance matrix is calculated by

$$Cov_c = \overline{Cov_L} + \overline{Cov_R}. \tag{3}$$

By eigenvalue decomposition, Cov_c is transformed into $Cov_c = E_c \lambda_c E_c'$, where E_c is eigenvector matrix of λ_c, and λ_c is the diagonal matrix of eigenvalues. With the whitening matrix

$$W = \sqrt{\lambda_c^{-1}} E_c', \tag{4}$$

$\overline{Cov_L}$ and $\overline{Cov_R}$ can be transformed into

$$S_L = W\overline{Cov_L}W' \quad \text{and} \quad S_R = W\overline{Cov_R}W'. \tag{5}$$

S_L and S_R share the same eigenvector matrix U, i.e.,

$$\text{if } S_L = U\lambda_L U' \quad \text{and } S_R = U\lambda_R U' \text{ then } \lambda_L + \lambda_R = I, \tag{6}$$

where I is the identity matrix, and the sum of eigenvalues of S_L and S_R is 1. After spatial filtering, the raw matrix M can be decomposed to

$$Z = PM, \tag{7}$$

where $P = U'W$ is the projection matrix. We used the variances of first m rows and last m rows of the new time series Z_i as the features, which can distinguish between the two classes best. The feature vector of i-th trial can be calculated as

$$f_j^i = \log\left(\frac{var_j^i}{\sum_{j=1}^{2m} var_j^i}\right), \tag{8}$$

where var_j^i is the variance of the j-th row of Z_i, $j = 1, 2 \ldots 2m$. One feature vector included $2m$ feature values (variances).

- *Classification:*
We applied linear discriminant analysis (LDA) [40], multi-layer perceptron (MLP) [41], Gaussian support vector machine (Gaussian SVM) [40], and sparse Bayesian extreme learning machine (SBELM) [42] which were commonly used in previous studies for EEG classification. The classification performance and computational time were compared and analyzed. For classification model, the inputs were feature vectors f_j^i of CSP, and the output was one of the two classes (Class L or Class R). All data (Class L and Class R) were separated into two parts: 80% data as training set and 20% data as testing set. To obtain more effective information and select the optimal model, 10-fold cross-validation was used in model training. Training set was separated into 9 folds for training and 1 fold for validation randomly.

2) STEP TWO: RECOGNIZE THE SPECIFIC MOVEMENT OF ONE ARM

After we got the classification result of Step one, EEG-EMG coherence was applied to recognize the specific movement of this arm. The raw EEG signals and EMG signals were filtered at 8-30 Hz. The filtered EEG signals of C3 and C4 and the filtered EMG signals of three muscles of this arm were extracted during second 3-7 (4-s time period after cue). Analysis of the EEG-EMG coherence was performed using 200-ms time segments with a 100-ms overlap (39 segments in 4 seconds).

- *Feature extraction:*
EEG-EMG coherence is helpful to understand the corticomuscular functional connection in muscle fatigue and motor recovery [27], [43]. In our work, EEG-EMG coherence was used as a feature in classification of different movements on one arm. By FFT with a 2-Hz frequency resolution, coherence between EEG (x) and EMG (y) can be expressed as

$$C_{xy}(f) = \frac{P_{xy}(f)}{P_{xx}(f) \times P_{yy}(f)}, \tag{9}$$

where $P_{xx}(f)$ is the autospectra of x at frequency f, $P_{yy}(f)$ is the autospectra of y at frequency f, and $P_{xy}(f)$

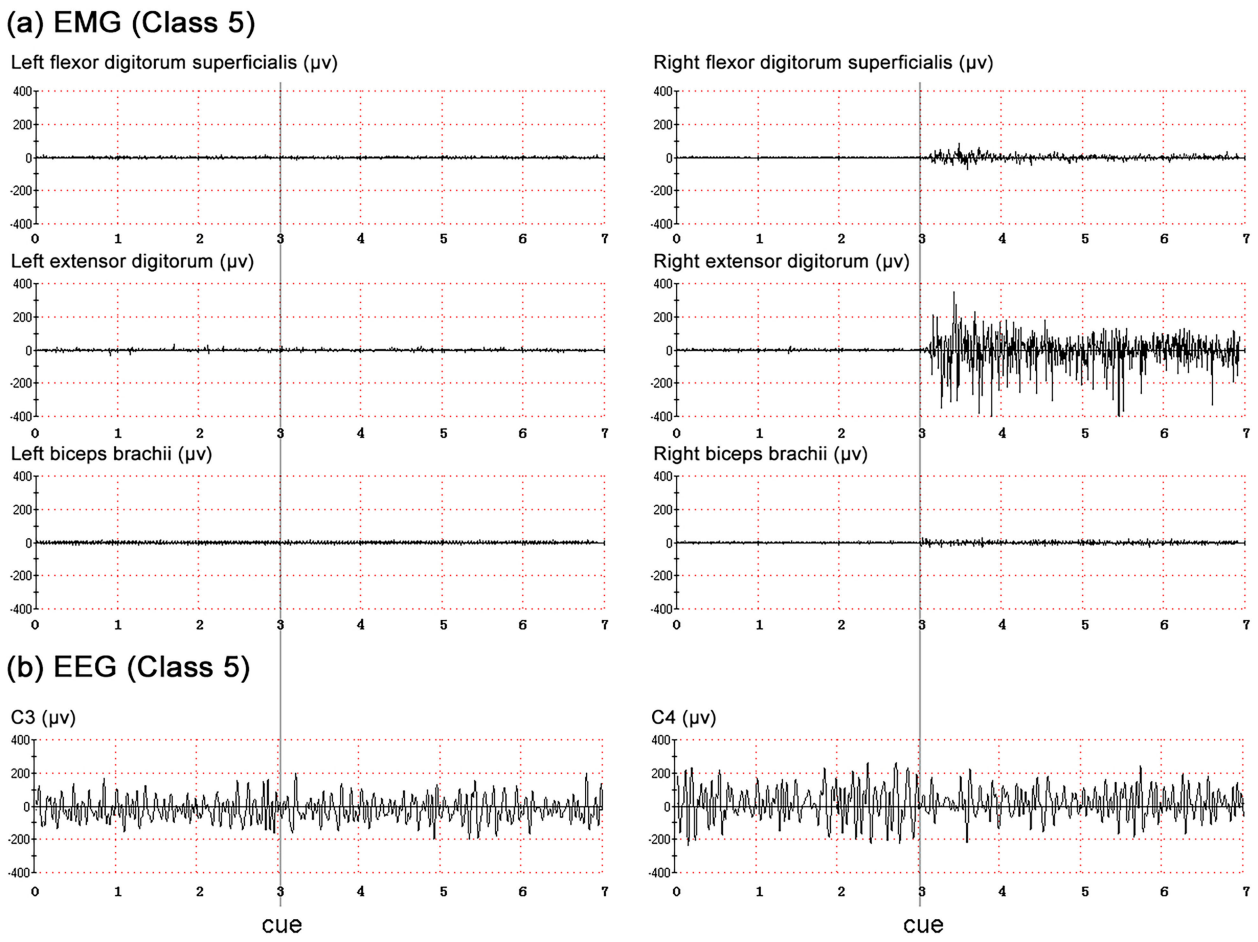

FIGURE 3. The raw EMG data (a) and EEG data (b) of one trial of Class 5 (Right-hand extension) obtained from a representative subject.

is the cross-spectrum between $P_{xx}(f)$ and $P_{yy}(f)$. $P_{xy}(f)$ is calculated as

$$P_{xy}(f) = \frac{1}{n}\sum_{s=1}^{n} x_s(f)y_s^*(f), \tag{10}$$

where $x_s(f)$ is the FFT of the s-th segment of EEG at frequency f, $y_s(f)$ is the FFT of the s-th segment of EMG at frequency f, n is the number of segments, and $*$ indicates complex conjugation. The range of coherence is 0 to 1, where 1 indicates a perfect linear relationship. If the value exceeded the $\alpha\%$ confidence limit, the coherence was considered to be significant. The $\alpha\%$ confidence limit can be calculated by the following equation

$$CL(\alpha) = 1 - (1 - \frac{\alpha}{100})^{\frac{1}{n-1}} \tag{11}$$

with α of 95% corresponding in this study to the confidence limits of 0.076 (n = 39). For each trial, totally 72 coherence values, i.e., 3 muscles × 2 EEG channels × 12 frequencies, formed the feature vector which was feeded into the classifier.

- *Classification:*
We applied the same four classifiers in Step one for EEG-EMG coherence classification. The classification performance and computational time were compared and analyzed. The inputs were the feature vectors from EEG-EMG coherence, and the output was one of the three classes of movements in one arm, i.e., make a left/right fist, left/right-hand extension, and left/right-elbow flexion. All data (Class L or Class R) were separated into two parts: 80% data as training set and 20% data as testing set. The same 10-fold cross-validation method in Step one was used in model training.

F. DATA ANALYSIS

In this study, accuracy was used for evaluation of classification models, calculating by

$$accuracy = \frac{TP + TN}{TP + TN + FP + FN}, \tag{12}$$

where TP means true positive, TN means true negative, FP means false positive and FN means false negative. Precision, recall and F-score were used for evaluation of classification performance of different classes. Precision shows the ratio of predicted TPs to all predicted positives, and recall shows the ratio of predicted TPs to all actual positives. They are

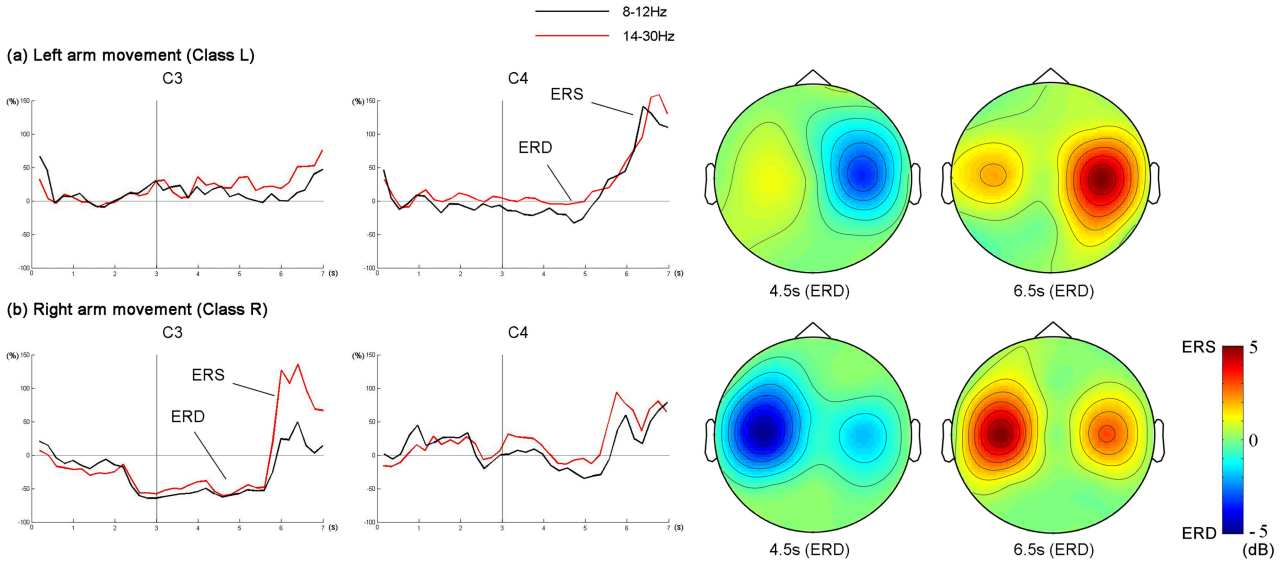

FIGURE 4. ERD/ERS curves (left side) and grand average topographies (right side) of left arm movement (a) and right arm movement (b).

calculated by

$$precision = \frac{TP}{TP + FP} \quad \text{and} \quad recall = \frac{TP}{TP + FN}. \quad (13)$$

As an extension of accuracy, F-score combines the precision and recall, which is expressed as

$$F - score = \frac{2 \times precision \times recall}{precision + recall}. \quad (14)$$

III. RESULTS

After experiment, trials including artifacts were excluded according to trial exclusion process. The remaining data were further analyzed and processed. The raw EEG data and EMG data of one trial of Class 5 (right-hand extension) obtained from a representative subject are shown in Figure 3. Figure 3(a) shows 7-second raw EMG records of six muscles in left and right arm. The subject performed right-hand extension movement, so we can see the extensor digitorum muscle activity in right arm. Figure 3(b) shows 7-second raw EEG records of C3 and C4 channels.

A. STEP ONE: DISTINGUISH BETWEEN LEFT AND RIGHT ARM MOVEMENT

1) NEUROPHYSIOLOGICAL ANALYSIS OF ERD/ERS

To visualize the ERD/ERS curves of Class L and Class R, EEG power of C3 and C4 channels within two frequency bands (8-12 Hz and 14-30 Hz) during 0-7 s are averaged over all trials and all subjects. The ERD/ERS curves are calculated as a percentage of EEG power decrease/increase relative to the reference period, and displayed in the left side of Figure 4. The ERD/ERS curves show a strong ERD and a closely following post-movement ERS over the contralateral area during second 4-7 (1-4 s after cue), while a weak ERS is observed over the ipsilateral area. Besides, ERD can be seen in both alpha and beta frequency bands, while ERS is more significant in beta bands. Then, the grand average topographies of alpha and beta bands at second 4.5 (ERD) and second 6.5 (ERS) are calculated for further analysis, as shown in the right side of Figure 4.

Figure 5 shows examples of time-frequency maps for left arm (Class L) and right arm (Class R) movements from four subjects. The time-frequency maps of C3 and C4 channels which display the best ERD/ERS are illustrated. The black lines at second 3 indicate the cue appearance. Blue color and red color represent the power decrease (ERD pattern) and power increase (ERS pattern), respectively. For S1, S2 and S4, ERD is found around second 4-6 (1-3 s after the cue) rather than from second 3 immediately because of the response delay, and post-movement ERS is found around second 6-7 when subjects stopped arm movements; ERD is observed in both alpha and beta frequency bands (8-30 Hz) over the contralateral sensorimotor area to the arm movements, and ERS is observed mainly in beta frequency band over the contralateral sensorimotor area to the arm movements. Comparing with ERD, ERS is short in duration but highly recognizable. However, ERD and ERS are less obvious for S3. According to the time-frequency maps, the optimal frequency band of each subject is: 10-14 Hz for S1, 12-16 Hz for S2, 16-22 Hz for S3 and 8-12 Hz for S4.

2) CLASSIFICATION RESULTS

For each subject, the optimal time period and frequency band of each subject were chosen to extract features and classify according to Figure 4 and Figure 5. Four classifiers (LDA, MLP, Gaussian SVM and SBELM) were trained to recognize the left arm movement or right arm movement. Figure 6 shows the confusion matrix and average accuracies of four classifiers over all subjects. The values of entries of

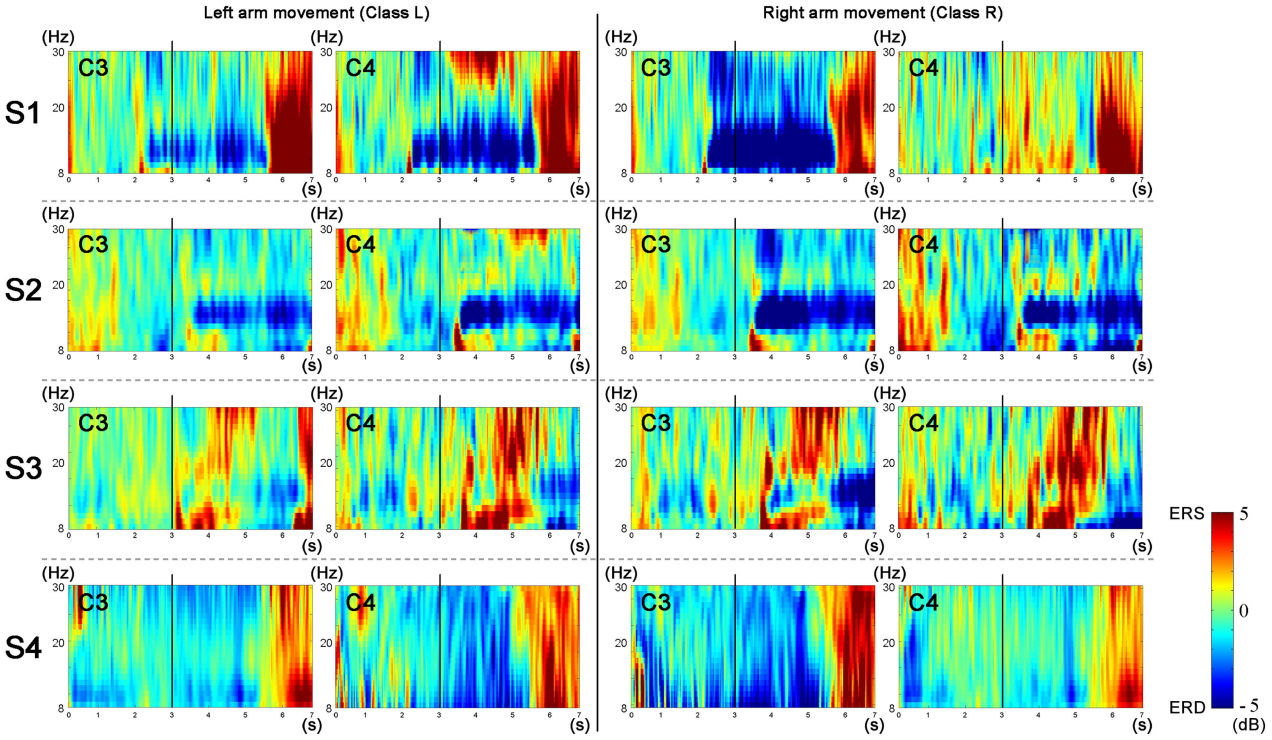

FIGURE 5. Examples of time-frequency maps for left arm (Class L) and right arm (Class R) movements from four subjects.

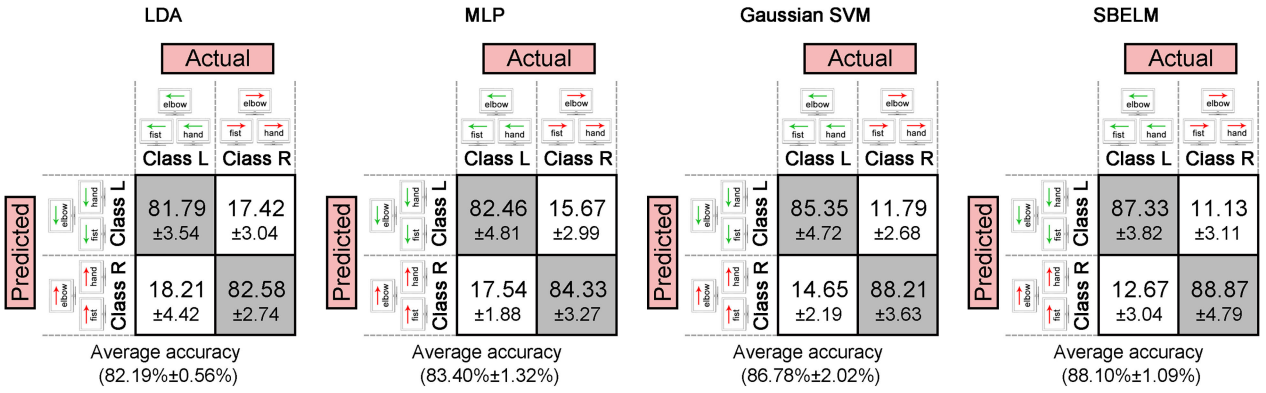

FIGURE 6. Confusion matrix and average accuracies of four classifiers (in %) in Step one over all subjects.

this matrix stand for average value ± standard deviation. The main diagonal and off-diagonal entries indicate the correct classification and the incorrect classification, respectively. SBELM and Gaussian SVM have a better classification performance than LDA and MLP in Step one. SBELM achieves a highest average classification accuracy of 88.10%±1.09% in Step one and is slightly higher than Gaussian SVM (86.78%±2.02%). The accuracies of right arm movement (82.58%±2.74%, 84.33%±3.27%, 88.21%±3.63% and 88.87%±4.79%, respectively) are higher than those of left arm movement (81.79%±3.54%, 82.46%±4.81%, 85.35%±4.72% and 87.33%±3.82%, respectively) in four classifiers. The average precisions, recalls and F-scores of two classes of four classifiers in Step one over all subjects are shown in Figure 7. The high precision and recall generally mean the good performance of the classifier (SBELM: average precision = 0.8811±0.0083, average recall = 0.8810±0.0109). The average F-score of SBELM is 0.8810±0.0013.

B. STEP TWO: RECOGNIZE THE SPECIFIC MOVEMENT OF ONE ARM

1) EEG-EMG COHERENCE ANALYSIS

After the classification result of Step one was obtained, we knew which arm moved. For each subject, the trials with

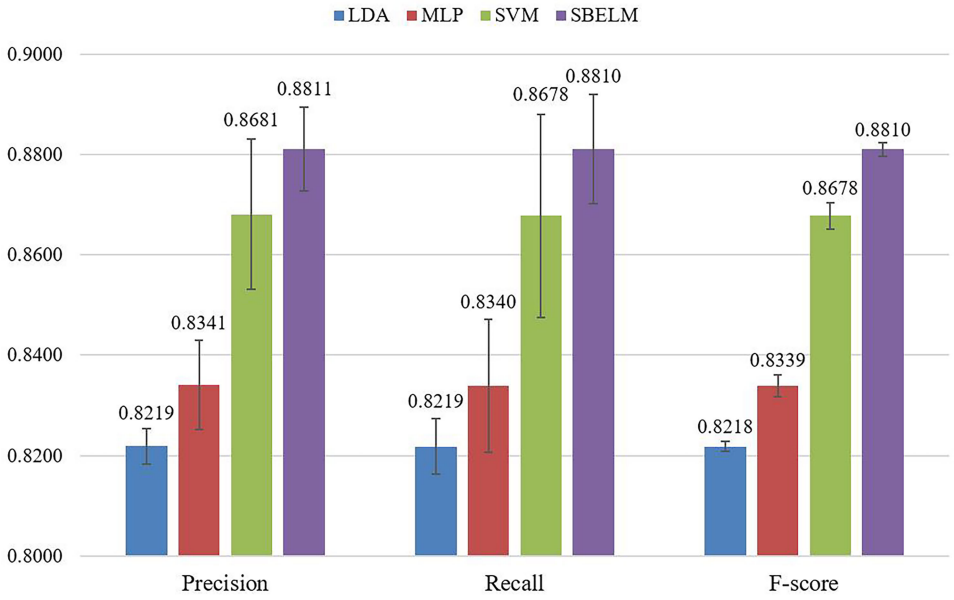

FIGURE 7. Average precisions, recalls and F-scores of two classes of four classifiers in Step one over all subjects.

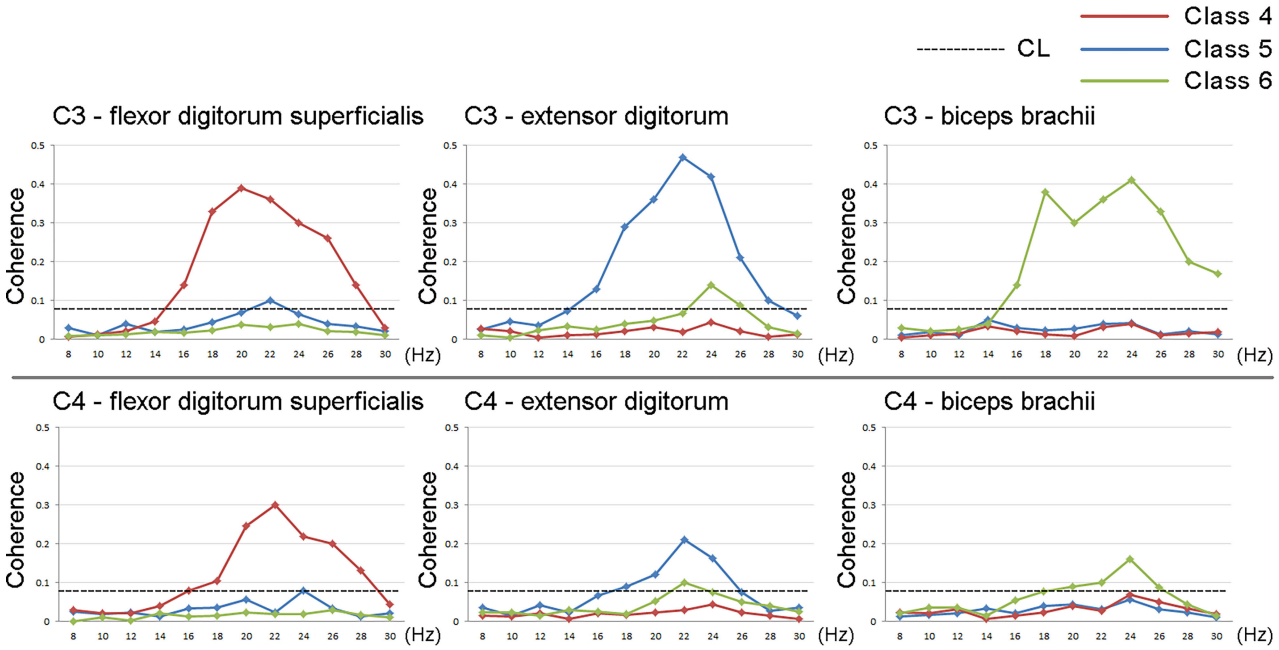

FIGURE 8. The EEG-EMG coherence of one trial of Class 4, Class 5 and Class 6 obtained from a representative subject.

correct classification in Step one proceeded to Step two. The raw EEG signal and EMG signal of each trial were filtered at 8-30 Hz. The filtered EEG signals of C3 and C4 and the filtered EMG signals of three muscles of this arm were extracted during second 3-7 (4-s time period after cue). EEG-EMG coherence was calculated with a 2-Hz frequency resolution. The data of one trial of Class 4, Class 5 and Class 6 obtained from a representative subject are shown in Figure 8. Coherence is considered to be significant if the value exceeds the confidence limit (0.076 in this study). For each class, only the coherence between C3/C4 and the corresponding agonistic muscle in the beta band (14-30Hz) is significant, i.e., C3/C4-flexor digitorum superficialis in Class 4 (peak value: 0.391(20Hz)/0.305(22Hz)), C3/C4-extensor digitorum in Class 5 (peak value: 0.475(22Hz)/0.218(22Hz)) and C3/C4-biceps brachii in Class 6 (peak value:

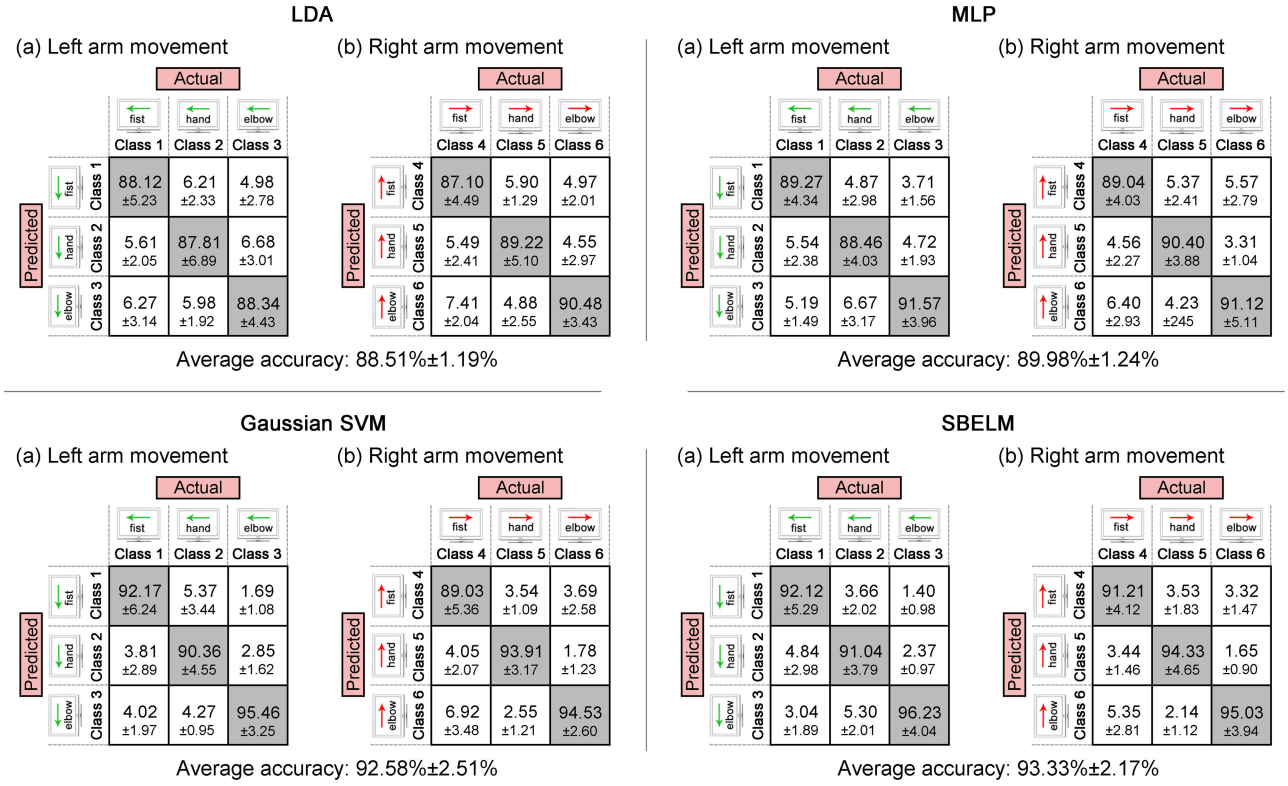

FIGURE 9. Confusion matrices (in %) of left arm and right arm movements and average accuracies of four classifiers in step two over all subjects.

0.419(24Hz)/0.164(24Hz)), respectively. Besides, for each class, the coherence between contralateral EEG channel (C3) and the corresponding agonistic muscle is more significant than the coherence between ipsilateral EEG channel (C4) and the corresponding agonistic muscle.

2) CLASSIFICATION RESULTS

EEG-EMG coherence across two EEG channels, three muscles and twelve frequencies was used as a feature in classification of Step two. For each subject, four classifiers were trained to classify different movements on one arm. Figure 9 shows the confusion matrices of left hand and right arm movements and average accuracies of four classifiers in Step two. SBELM and Gaussian SVM have a better classification performance than LDA and MLP in Step two. SBELM achieves a highest average classification accuracy of 93.33%±2.17% in Step one and is slightly higher than Gaussian SVM (92.58%±2.51%). The accuracies of elbow flexion movement (Class 3: 88.34%±4.43%, 91.57%±3.96%, 95.46%±3.25% and 96.23%±4.04%, respectively; Class 6: 90.48%±3.43%, 91.12%±5.11%, 94.53%±2.60% and 95.03%±3.94%, respectively) are higher than those of other two movements for both sides in all four classifiers. There is no significant different between the accuracy of left arm movement and the accuracy of right arm movement through t-test ($p > 0.05$). The average precisions, recalls and F-scores of six classes of four classifiers in Step two over all subjects are shown in Figure 10. SBELM achieves the higher average precision (0.9334±0.0120) and average recall (0.9349±0.0246) than the other three classifiers. The average F-score of SBELM is 0.9340±0.0119. Step two does extremely well in classifying right hand extension (Class 5, F-score: 0.8955, 0.9119, 0.9403 and 0.9460, respectively) in four classifiers. Movements such as make a left fist (Class 1, F-score: 0.8843, 0.9024, 0.9253 and 0.9344, respectively), left elbow flexion (Class 3, F-score: 0.8808, 0.9003, 0.9370 and 0.9456, respectively) and right elbow flexion (Class 6, F-score: 0.8924, 0.9033, 0.9268 and 0.9385, respectively) also are detected very well in four classifiers. Combining the best classifier which achieves the best classification performance in Step one and Step two, we get a final accuracy of 82.22% (average accuracy using SBELM in Step one $\times$ average accuracy using SBELM in Step two) for this two-step single-trial classification method.

IV. DISCUSSION

By using EEG related to natural motions, we can combine human brain with external environment, not only for healthy users, but for patients with neuromuscular disorder. EEG is useful to distinguish between left arm and right arm movements, however, it is difficult to classify the different movements on one arm. For solving this problem, we proposed a two-step single-trial classification method in this study.

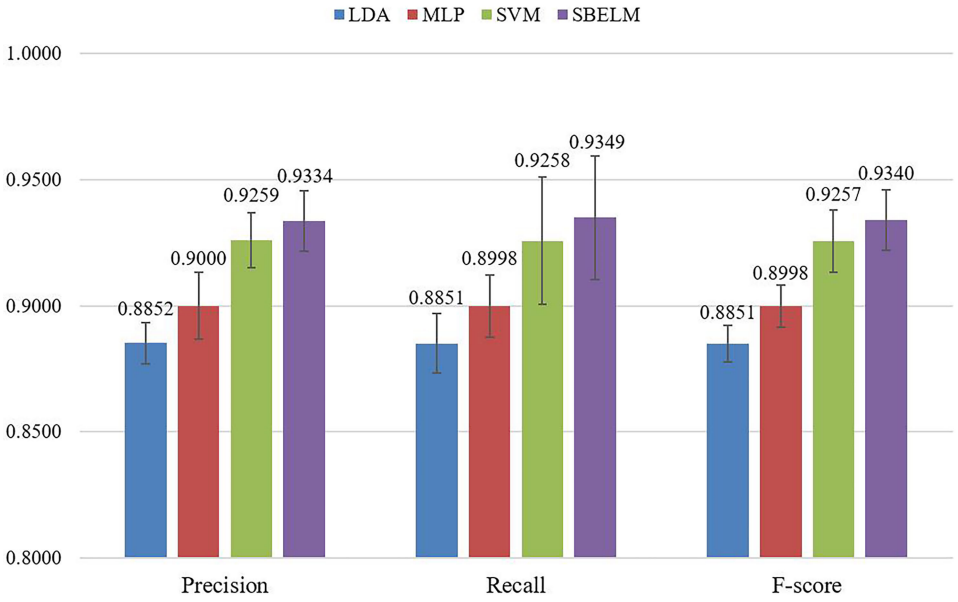

FIGURE 10. Average precisions, recalls and F-scores of six classes of four classifiers in Step two over all subjects.

In Step one, we used ERD/ERS patterns to distinguish between left arm and right arm movements. We observed a strong ERD over the contralateral area and a week ERS over the ipsilateral area during the arm movements, and a strong post-movement ERS when subjects stopped arm movements. ERD can be seen in both alpha and beta frequency bands, while ERS is more significant in beta bands. The reason of these facts is that the underlying neuronal populations synchrony will be low during ME or MI, resulting in an ERD; the motor cortex networks will deactivate (inhibit) and/or reset when the ME or MI stops (post-movement), resulting in a short-live ERS [15], [16]. As shown in Figure 4, ERD can be seen in both alpha and beta frequency bands (8-30 Hz), while ERS is more significant in beta bands. As shown in Figure 5, ERD and ERS over the contralateral and ipsilateral sensorimotor areas were highly recognizable for S1, S2 and S4, while they were less obvious for S3. The possible reason is that S3 belongs to the portion of ''BCI Illiteracy'' user (estimated 15-30%) who do not show the expected sensorimotor rhythms [44]. Besides, the contralateral ERD pattern were more obvious during right arm movement than during left arm movement. This may be because all subjects were right handed. Since the cortical control mechanisms are different between dominant hand and non-dominant hand, ERD at alpha and beta frequency bands occur over the contralateral sensorimotor area when dominant hand moves, whereas over the bilateral sensorimotor areas when non-dominant hand moves [45]. After extracting features from ERD/ERS patterns by CSP, four classifiers were trained, and achieved a best classification accuracy of 88.10%±1.09%.

After we obtained the classification result of Step one, EEG-EMG coherence was applied to recognize the specific movement of this arm in Step two. For each class, only the coherence between C3/C4 and the corresponding agonistic muscle in the beta band (14-30Hz) was significant, as shown in Figure 8. This is because each movement in this study only leads to the corresponding agonistic muscle contraction, i.e., flexor digitorum superficialis contraction in Class 1 and 4, extensor digitorum contraction in Class 2 and 5 and biceps brachii contraction in Class 3 and 6. During the agonistic muscle contraction, functional coupling between cortex and this muscle in time and frequency domains is revealed by calculating the coherence between EEG and EMG, but no functional coupling between cortex and other muscles is found [26]. The differentiable EEG-EMG coherence values of each class formed the feature vector and achieved a well performance (the best average accuracy is 93.33%±2.17%) in classification of different movements on one arm. According to Figure 9, the accuracies of elbow flexion movement are higher than those of other two movements for both sides. The possible reason is that the elbow flexion movement has a stronger functional coupling relationship than the other two movements, resulting in the better EEG-EMG coherence features for classification.

In our experiment, we compared four classifiers in Step one and Step two. Gaussian SVM and SBELM achieved the better classification performance than LDA and MLP. This probably is due to their regularization property and their immunity to the curse-of-dimensionality [41]. SBELM achieved a highest average classification accuracy and was slightly higher than Gaussian SVM in two steps, which leaded to the best final accuracy of 82.22%. This may be because SBELM is able to automatically exclude redundant hidden neurons and derive a compact model with high generalization capability

TABLE 2. Average computational time of two steps and total time of four classifiers (s) over all subjects.

	Step one	Step two	total time
LDA	2.45±0.25	2.96±0.31	5.41±0.39
MLP	3.03±0.22	3.55±0.28	6.58±0.49
Gaussian SVM	19.89±0.68	20.75±0.95	40.64±1.12
SBELM	2.45±0.20	2.07±0.35	4.05±0.44

for further improving EEG classification [42]. We also compared the computational time of four classifiers during model training in Step one and Step two. This was done under MATLAB R2017a on a Windows laptop with 2.5 GHz CPU. As shown in Table 2, LDA, MLP and SBELM (total time: 5.41s±0.39s, 6.58s±0.49s and 4.05s±0.44s, respectively) took much shorter time than Gaussian SVM (total time: 40.64s±1.12s). Overall, SBELM was the optimal classifier in our study because of the high classification performance and computational efficiency.

The classification performance using EEG-EMG coherence to classify different movements on one arm is much better than that using only EEG features in some existing studies. Quandt *et al.* [25] used spatiotemporal patterns in the time series of EEG to classify four finger movements (press button with four different fingers) in one hand, only resulting in an average accuracy of 43% over all subjects. Most of these research mainly focused on the feature optimization and classification algorithms of EEG. In some new feature extraction methods, filter bank strategy can design filter banks to decompose MI EEG into different frequency bands and obtain the optimal frequency band through feature selection method [46]; temporally constrained sparse group spatial patterns (TSGSP) can simultaneously optimize filter bands and time window within CSP to further boost classification accuracy of MI EEG [47]; deep learning method, like convolutional neural network (CNN), directly faces to the raw signal and helps to extract the most discriminant features (high-level features) for MI EEG classification based on receptive field and weight sharing [48]. Some new classification methods, like sparse representation-based classification (SRC) scheme and sparse group representation model (SGRM), outperform the conventional classifiers and improve the efficiency of MI-based BCI [49]. The effectiveness of these method have been verified, but they cannot fundamentally improve the classification performance of different movements on one arm. The reason is that non-invasive EEG is a signal with low signal-to-noise ratio and limited spatiotemporal resolution, and may be insufficient to recognize the weak changes of different movements on one arm. Therefore, an additional input information (EMG) was applied in this study. According to the classification performance of Step two, we verified that using EEG-EMG coherence can classify different movements on one arm effectively. However, these feature optimization and classification algorisms may affect the classification performance of our proposed method. The other existing studies on classification of different movements on one arm used EMG or/and motion information (angle, acceleration, etc.). One advantage of our method in comparison with these methods is that subjects were not required to perform movements in a fixed velocity or fixed force (but did it naturally), because the magnitude of force in mild level and moderate level will not affect the EEG-EMG coherence [50]. This fact lets our method be applicable in muscle weakness or stroke patients who cannot provide the completed EMG signals or motion information but can still move their arms. It is also the reason why we don't use only EMG in our study.

EEG artifacts of blinks, eye movements or body movements may affect BMI applications seriously [51]. During the ME experiment, a camera was used to observe subjects to ensure that they did not make unnecessary movements (eye or tongue movements) and correct movements were performed. In addition, after the experiment, we identified all trials offline and excluded the trials including the EEG and EMG artifacts from the following analyses. These two operations ensured the data used for analysis without the artifact contamination.

Previous studies proved that muscle fatigue can affect EMG signals seriously [52]. To avoid this, subjects had a rest of 5-10 minutes between every 60 trials in our experiment. Furthermore, subjective stop and objective observation were applied to ensure fatigue-free data. Although the effect of muscle fatigue is not our focus of this paper, it is still necessary to do the fatigue test.

Our future work covers the following two aspects to address limitations in this study: (1) feature optimization/selection and classification algorisms are not our focus of this paper, but these methods may affect the classification performance. Some new feature extraction methods (like filter bank strategy, TSGSP and deep learning), and some new classifiers (like SRC scheme and SGRM) will be investigated further. (2) The current results demonstrate that our method are applicable to the classification of different movements on one arm for healthy and young adults, but BMI is also applied in patients affected by motor disabilities and various age groups. Therefore, an extensive testing on these people will be planned in our future studies.

V. CONCLUSION

In summary, our findings help solve an important problem of different movements classification on one arm. A two-step single-trial classification method is proposed to recognize three movements (make a fist, hand extension and elbow flexion) of left and right arms: (1) distinguish between left hand and right arm movements by decoding ERD/ERS and (2) recognize the specific movement of this arm using EEG-EMG coherence as features. The classification results show the accuracy of Step one and Step two is 88.10% and 93.33%, respectively. This proposed method achieves a total accuracy of 82.22%. This study demonstrates that our method is effective to classify different movements on one arm, and provides the theoretic basis and technical support for the practical development of BMI-based motor restoration applications.

REFERENCES

[1] A. R. C. Donati, S. Shokur, E. Morya, D. S. F. Campos, R. C. Moioli, C. M. Gitti, P. B. Augusto, S. Tripodi, C. G. Pires, G. A. Pereira, F. L. Brasil, S. Gallo, A. A. Lin, A. K. Takigami, M. A. Aratanha, S. Joshi, H. Bleuler, G. Cheng, A. Rudolph, and M. A. L. Nicolelis, "Long-term training with a brain-machine interface-based gait protocol induces partial neurological recovery in paraplegic patients," *Sci. Rep.*, vol. 6, Aug. 2016, Art. no. 30383.

[2] X. Zhao, J. Zhao, W. Cai, and S. Wu, "Transferring common spatial filters with semi-supervised learning for zero-training motor imagery brain-computer interface," *IEEE Access*, vol. 7, pp. 58120–58130, 2019.

[3] A. B. Remsik *et al.*, "Ipsilesional Mu rhythm desynchronization and changes in motor behavior following post stroke BCI intervention for motor rehabilitation," *Frontiers Neurosci.*, vol. 13, pp. 1–18, Mar. 2019.

[4] Z. Chen, Z. Wang, K. Wang, W. Yi, and H. Qi, "Recognizing motor imagery between hand and forearm in the same limb in a hybrid brain computer interface paradigm: An online study," *IEEE Access*, vol. 7, pp. 59631–59639, 2019.

[5] A. Biasiucci, R. Leeb, I. Iturrate, S. Perdikis, A. Al-Khodairy, T. Corbet, A. Schnider, T. Schmidlin, H. Zhang, D. Viceic, P. Vuadens, A. G. Guggisberg, J. D. R. Millán, and M. Bassolino, "Brain-actuated functional electrical stimulation elicits lasting arm motor recovery after stroke," *Nature Commun.*, vol. 9, no. 1, 2018, Art. no. 2421.

[6] M. Dai, S. Wang, D. Zheng, R. Na, and S. Zhang, "Domain transfer multiple kernel boosting for classification of EEG motor imagery signals," *IEEE Access*, vol. 7, pp. 49951–49960, 2019.

[7] M. S. Fifer, G. Hotson, B. Wester, D. P. McMullen, Y. Wang, M. S. Johannes, K. D. Katyal, J. B. Helder, M. P. Para, and R. J. Vogelstein, "Simultaneous neural control of simple reaching and grasping with the modular prosthetic limb using intracranial EEG," *IEEE Trans. Neural Syst. Rehabil. Eng.*, vol. 22, no. 3, pp. 695–705, May 2014.

[8] V. D. Bohbot, M. S. Copara, J. Gotman, and A. D. Ekstrom, "Low-frequency theta oscillations in the human hippocampus during real-world and virtual navigation," *Nature Commun.*, vol. 8, Feb. 2017, Art. no. 14415.

[9] D. Huang, K. Qian, D.-Y. Fei, W. Jia, X. Chen, and O. Bai, "Electroencephalography (EEG)-based brain–computer interface (BCI): A 2-D virtual wheelchair control based on event-related desynchronization/synchronization and state control," *IEEE Trans. Neural Syst. Rehabil. Eng.*, vol. 20, no. 3, pp. 379–388, May 2012.

[10] A. K. Das, S. Suresh, and N. Sundararajan, "A discriminative subject-specific spatio-spectral filter selection approach for EEG based motor-imagery task classification," *Expert Syst. Appl.*, vol. 64, pp. 375–384, Dec. 2016.

[11] S. D. Stavisky, J. C. Kao, P. Nuyujukian, C. Pandarinath, C. Blabe, S. I. Ryu, L. R. Hochberg, J. M. Henderson, and K. V. Shenoy, "Brain-machine interface cursor position only weakly affects monkey and human motor cortical activity in the absence of arm movements," *Sci. Rep.*, vol. 8, no. 1, 2018, Art. no. 16357.

[12] H. Ramoser, J. Müller-Gerking, and G. Pfurtscheller, "Optimal spatial filtering of single trial EEG during imagined hand movement," *IEEE Trans. Neural Syst. Rehabil. Eng.*, vol. 8, no. 4, pp. 441–446, Dec. 2000.

[13] Y. Zhang, G. Zhou, J. Jin, Q. Zhao, X. Wang, and A. Cichocki, "Sparse Bayesian classification of EEG for brain–computer interface," *IEEE Trans. Neural Netw. Learn. Syst.*, vol. 27, no. 11, pp. 2256–2267, Nov. 2016.

[14] Y. Yang, S. Chevallier, J. Wiart, and I. Bloch, "Time-frequency optimization for discrimination between imagination of right and left hand movements based on two bipolar electroencephalography channels," *EURASIP J. Adv. Signal Process.*, vol. 2014, no. 1, 2014, Art. no. 38.

[15] G. Pfurtscheller and F. L. Da Silva, "Event-related EEG/MEG synchronization and desynchronization: Basic principles," *Clin. Neurophysiol.*, vol. 110, no. 11, pp. 1842–1857, 1999.

[16] G. Pfurtscheller and T. Solis-Escalante, "Could the beta rebound in the EEG be suitable to realize a 'brain switch?'" *Clin. Neurophysiol.*, vol. 120, no. 1, pp. 24–29, 2009.

[17] C. Neuper, R. Scherer, S. Wriessnegger, and G. Pfurtscheller, "Motor imagery and action observation: Modulation of sensorimotor brain rhythms during mental control of a brain–computer interface," *Clin. Neurophysiol.*, vol. 120, no. 2, pp. 239–247, Feb. 2009.

[18] G. Pfurtscheller, C. Neuper, D. Flotzinger, and M. Pregenzerb, "EEG-based discrimination between imagination of right and left hand movement," *Electroencephalogr. Clin. Neurophysiol.*, vol. 103, no. 6, pp. 642–651, Dec. 1997.

[19] D. Huang, P. Lin, D.-Y. Fei, X. Chen, and O. Bai, "Decoding human motor activity from EEG single trials for a discrete two-dimensional cursor control," *J. Neural Eng.*, vol. 6, no. 4, 2009, Art. no. 046005.

[20] O. Bai, P. Lin, S. Vorbach, M. K. Floeter, N. Hattori, and M. Hallett, "A high performance sensorimotor beta rhythm-based brain–computer interface associated with human natural motor behavior," *J. Neural Eng.*, vol. 5, no. 1, pp. 24–35, 2008.

[21] B. J. Edelman, B. Baxter, and B. He, "EEG source imaging enhances the decoding of complex right-hand motor imagery tasks," *IEEE Trans. Biomed. Eng.*, vol. 63, no. 1, pp. 4–14, Jan. 2016.

[22] I. R. Minev, P. Musienko, A. Hirsch, Q. Barraud, N. Wenger, E. M. Moraud, J. Gandar, M. Capogrosso, T. Milekovic, and L. Asboth, "Electronic dura mater for long-term multimodal neural interfaces," *Science*, vol. 347, no. 6218, pp. 159–163, 2015.

[23] S. R. Soekadar, M. Witkowski, C. Gómez, E. Opisso, J. Medina, M. Cortese, M. Cempini, M. C. Carrozza, L. G. Cohen, N. Birbaumer, and N. Vitiello, "Hybrid EEG/EOG-based brain/neural hand exoskeleton restores fully independent daily living activities after quadriplegia," *Sci. Robot.*, vol. 1, no. 1, 2016, Art. no. eaag3296.

[24] M. Rodríguez-Ugarte, E. Iáñez, M. Ortiz, and J. M. Azorín, "Improving real-time lower limb motor imagery detection using tDCS and an exoskeleton," *Frontiers Neurosci.*, vol. 12, p. 757, Oct. 2018.

[25] F. Quandt, C. Reichert, H. Hinrichs, H. J. Heinze, R. T. Knight, and J. W. Rieger, "Single trial discrimination of individual finger movements on one hand: A combined MEG and EEG study," *NeuroImage*, vol. 59, no. 4, pp. 3316–3324, 2012.

[26] T. Mima and M. Hallett, "Corticomuscular coherence: A review," *J. Clin. Neurophysiol.*, vol. 16, no. 6, pp. 501–511, 1999.

[27] T. Mima, K. Toma, B. Koshy, and M. Hallett, "Coherence between cortical and muscular activities after subcortical stroke," *Stroke*, vol. 32, no. 11, pp. 2597–2601, Nov. 2001.

[28] P. C. Poortvliet, K. J. Tucker, S. Finnigan, D. Scott, and P. W. Hodges, "Experimental pain decreases corticomuscular coherence in a force-but not a position-control task," *J. Pain*, vol. 2, pp. 192–200, Feb. 2018.

[29] K. von Carlowitz-Ghori, Z. Bayraktaroglu, G. Waterstraat, G. Curio, and V. V. Nikulin, "Voluntary control of corticomuscular coherence through neurofeedback: A proof-of-principle study in healthy subjects," *Neuroscience*, vol. 290, pp. 243–254, Apr. 2015.

[30] T. Mima, S. Ohara, and T. Nagamine, "Cortical–muscular coherence," in *International Congress Series*, vol. 1226. Amsterdam, The Netherlands: Elsevier, 2002, pp. 109–119.

[31] R. C. Oldfield, "The assessment and analysis of handedness: The Edinburgh inventory," *Neuropsychologia*, vol. 9, no. 1, pp. 97–113, 1971.

[32] Z. Tang, S. Sun, S. Zhang, Y. Chen, C. Li, and S. Chen, "A brain-machine interface based on ERD/ERS for an upper-limb exoskeleton control," *Sensors*, vol. 16, no. 12, p. 2050, 2016.

[33] A. Luttmann, M. Jäger, J. Sökeland, and W. Laurig, "Electromyographical study on surgeons in urology. II. Determination of muscular fatigue," *Ergonomics*, vol. 39, no. 2, pp. 298–313, 1996.

[34] M. J. M. Hoozemans and J. H. van Dieën, "Prediction of handgrip forces using surface EMG of forearm muscles," *J. Electromyogr. Kinesiol.*, vol. 15, no. 4, pp. 358–366, 2005.

[35] A. Smith and E. E. Brown, "Myoelectric control techniques for a rehabilitation robot," *Appl. Bionics Biomech.*, vol. 8, no. 1, pp. 21–37, 2011.

[36] J. V. Basmajian, *Biofeedback: Principles and Practice for Clinicians*. Baltimore, MD, USA: Williams & Wilkins, 1979.

[37] O. Bai, Z. Mari, S. Vorbach, and M. Hallett, "Asymmetric spatiotemporal patterns of event-related desynchronization preceding voluntary sequential finger movements: A high-resolution EEG study," *Clin. Neurophysiol.*, vol. 116, no. 5, pp. 1213–1221, 2005.

[38] G. Onose, C. Grozea, A. Anghelescu, C. Daia, C. Sinescu, A. V. Ciurea, T. Spircu, A. Mirea, I. Andone, A. Spânu, C. Popescu, A.-S. Mihaescu, S. Fazli, M. Danóczy, and F. Popescu, "On the feasibility of using motor imagery EEG-based brain–computer interface in chronic tetraplegics for assistive robotic arm control: A clinical test and long-term post-trial follow-up," *Spinal Cord*, vol. 50, no. 8, pp. 599–608, 2012.

[39] S. Lemm, B. Blankertz, G. Curio, and K.-R. Müller, "Spatio-spectral filters for improving the classification of single trial EEG," *IEEE Trans. Biomed. Eng.*, vol. 52, no. 9, pp. 1541–1548, Sep. 2005.

[40] S. Aditya and D. N. Tibarewala, "Comparing ANN, LDA, QDA, KNN and SVM algorithms in classifying relaxed and stressful mental state from two-channel prefrontal EEG data," *Int. J. Artif. Intell. Soft Comput.*, vol. 3, no. 2, pp. 143–164, 2012.

[41] F. Lotte, M. Congedo, A. Lécuyer, F. Lamarche, and B. Arnaldi, "A review of classification algorithms for EEG-based brain–computer interfaces," *J. Neural Eng.*, vol. 4, no. 2, pp. 1–13, 2007.
[42] Z. Jin, G. Zhou, D. Gao, and Y. Zhang, "EEG classification using sparse Bayesian extreme learning machine for brain–computer interface," *Neural Comput. Appl.*, vol. 10, pp. 1–9, Oct. 2018.
[43] J. Ushiyama, M. Katsu, Y. Masakado, A. Kimura, M. Liu, and J. Ushiba, "Muscle fatigue-induced enhancement of corticomuscular coherence following sustained submaximal isometric contraction of the tibialis anterior muscle," *J. Appl. Physiol.*, vol. 110, no. 5, pp. 1233–1240, 2011.
[44] C. Vidaurre and B. Blankertz, "Towards a cure for BCI illiteracy," *Brain Topogr.*, vol. 23, no. 2, pp. 194–198, Jun. 2010.
[45] K. Yamanaka, "Performance and cortical EEG dynamics during bimanual go/stop tasks in right- and left-handed individuals," *Int. J. Psychophysiol.*, vol. 2, no. 94, pp. 254–263, 2014.
[46] K. K. Ang and C. Guan, "EEG-based strategies to detect motor imagery for control and rehabilitation," *IEEE Trans. Neural Syst. Rehabil. Eng.*, vol. 25, no. 4, pp. 392–401, Apr. 2017.
[47] Y. Zhang, C. S. Nam, G. Zhou, J. Jin, X. Wang, and A. Cichocki, "Temporally constrained sparse group spatial patterns for motor imagery BCI," *IEEE Trans. Cybern.*, vol. 49, no. 9, pp. 3322–3332, Sep. 2018.
[48] Z. Tang, C. Li, and S. Sun, "Single-trial EEG classification of motor imagery using deep convolutional neural networks," *Optik-Int. J. Light Electron Opt.*, vol. 130, pp. 11–18, Feb. 2017.
[49] Y. Jiao, Y. Zhang, X. Chen, E. Yin, J. Jin, X. Wang, and A. Cichocki, "Sparse group representation model for motor imagery EEG classification," *IEEE J. Biomed. Health Inform.*, vol. 23, no. 2, pp. 631–641, Mar. 2019.
[50] T. Mima, N. Simpkins, T. Oluwatimilehin, and M. Hallett, "Force level modulates human cortical oscillatory activities," *Neurosci. Lett.*, vol. 275, no. 2, pp. 77–80, 1999.
[51] D. J. McFarland, W. A. Sarnacki, T. M. Vaughan, and J. R. Wolpaw, "Brain-computer interface (BCI) operation: Signal and noise during early training sessions," *Clin. Neurophysiol.*, vol. 116, no. 1, pp. 56–62, 2005.
[52] R. M. Enoka, S. Baudry, T. Rudroff, D. Farina, M. Klass, and J. Duchateau, "Unraveling the neurophysiology of muscle fatigue," *J. Electromyogr. Kinesiol.*, vol. 21, no. 2, pp. 208–219, 2011.

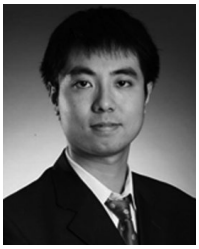

ZHICHUAN TANG received the Ph.D. degree in computer science and technology from Zhejiang University, China. He was a Postdoctoral Researcher with Bournemouth University, U.K. He is currently an Associate Professor with the Zhejiang University of Technology. He was an Erasmus Mundus Scholar in 2014. He has published more than 30 international journals and conference research articles. He is an Active Member of CCF and CAA. His research interests include brain-computer interaction, artificial intelligence, deep learning, intelligent ergonomics, and human–computer interaction. He is a Reviewer of TNSRE, TIE, IJIE, and *Sensors*.

HONGNIAN YU received the B.S. degree in automation from the Harbin Institute of Technology, Harbin, China, in 1982, the M.S. degree in automation from the Northeast Heavy Machinery College, Yanshan University, Qinhuangdao, China, in 1985, and the Ph.D. degree in mechanical engineering from London University, London, U.K., in 1994.

He has held academic positions with the University of Sussex, Brighton, U.K., Liverpool John Moor University, Liverpool, U.K., the University of Exeter, Exeter, U.K., the University of Bradford, Bradford, U.K., Staffordshire University, Stoke-on-Trent, U.K., Bournemouth University, Poole, U.K. He is currently with Edinburgh Napier University, Edinburgh, U.K. He has published more than 200 journals and conference research articles. His current research interests include large discrete event dynamic systems, networked control systems, and robotics.

Dr. Yu was a recipient of the Gold Medal on the World Exhibition on Inventions, Research and New Technologies, INNOVA 2009, Brussels, and the International Exhibition of Inventions, Geneva, Switzerland, in 2010, and the China Association of Inventors (CAI) Award at the 43rd International Exhibition of Inventions, New Techniques and Products, Geneva, in 2015.

CHUNFU LU is currently a Professor with the Industrial Design Institute, Zhejiang University of Technology. He has published more than 20 journal articles and holds more than 20 patents. His research interests include intelligent design, human factors, and human–computer interface.

PENGCHENG LIU is currently a Senior Lecturer with the Cardiff School of Technologies, Cardiff Metropolitan University, U.K. He has published more than 50 journals and conference research articles. His research interests include robotics, machine learning, and control systems. He is an Active Member of the IEEE Robotics and Automation Society. He received the Outstanding Contribution Awards from Elsevier, in 2017. He is an Associate Editor of IEEE Access. He is a regular Funding/Grants Reviewer for EPSRC, NIHR, and NSFC.

XUEXUE JIN is currently pursuing the master's degree with the Industrial Design Institute, Zhejiang University of Technology. Her research interests include intelligent design, human factors, and human–computer interface.